Probabilistic properties of ranges of sums in dynamical systems

H. Van de Vyver and C. Nicolis
Institut Royal Météorologique de Belgique, 3 Avenue Circulaire, B-1180 Brussels, Belgium
(Received 2 April 2010; revised manuscript received 1 July 2010; published 3 September 2010)

The principal signatures of deterministic dynamics in the statistical properties of the range and normalized range of sums are identified. Substantial differences from the classical statistical theory are found. Analytical expressions are derived, compared to those of the classical theory, and applied to generic classes of dynamical systems giving rise to chaotic and intermittent chaotic behavior.

DOI: 10.1103/PhysRevE.82.031107 PACS number(s): 02.50.−r, 05.45.−a, 05.20.−y

I. INTRODUCTION

Extreme events are a key manifestation of complex systems and their technological, economic and social consequences are a matter of considerable concern. There is a vast literature on the statistical description of extreme events which may be regarded as a well established area of investigation [1,2]. The classical version is based on the assumption of independent and identically distributed random variables (iidrv's). An excellent overview of the theory of extreme values for a wide class of correlated stochastic sequences is provided in [3]. More recently, theoretical advances have been made for the study of extreme events in deterministic dynamical systems [4–8].

In many environmental recordings the variability is so considerable that no underlying regularity seems to be present. An ingenious way to handle such records was suggested some time ago by Hurst [9]. The starting point is the sequence $X_0,\ldots,X_{n-1}$ of values of the variable of interest. The sample mean and the standard deviation of this record are denoted by $\bar{X}_n$ and C_n, respectively (we assume that the X_i's have a finite variance). Subtracting $\bar{X}_n$ from each of the values of the record leads to a new sequence of variables that have zero mean,

$$x_0 = X_0 - \bar{X}_n, \ldots, x_{n-1} = X_{n-1} - \bar{X}_n. \tag{1}$$

Next, we form partial sums of these variables, each of them being the cumulative sum of all values up to a particular value x_k,

$$S_1 = x_0, S_2 = x_0 + x_1, \ldots, S_n = x_0 + \ldots + x_{n-1}. \tag{2}$$

The set of these sums, noting that $S_n=0$, will have a maximum and a minimum value, $M_n=\max S_k$, $m_n=\min S_k$, when the k's run up to n. The range, r_n, of the phenomenon described by the sequence is then quite naturally defined as

$$r_n = M_n - m_n, \tag{3a}$$

or, in rescaled form,

$$r_n^* = r_n/C_n. \tag{3b}$$

In a complex system one expects that r_n should display a pronounced variability. To sort out systematic trends one should thus compute its average value or perhaps a higher moment thereof. The basic quality involved in such an averaging is the probability distribution of the event

$$F(u,v,n) = \mathrm{Prob}(M_n \le u, m_n \ge -v, n) \tag{4}$$

where u and v are taken to be positive, $M_n>0$ and $m_n<0$.

Closely related to the foregoing is the Hurst phenomenon. Specifically, a surprising result is that in a wide range of environmental records, $\langle r_n^* \rangle \sim n^H$, where H (referred to as the Hurst exponent) turns out to be close to 0.7. To put this in perspective, Feller [10] proved that for the reference case of iidrv's, H is bound to be 0.5. This implies in turn that the successive X's are not independent: S_k has somehow a persistent effect on X_k, i.e., highs tend to be followed by highs, lows by lows. This remarkable property discovered by Hurst has fascinated mathematicians, statisticians, physicists, engineers, and hydrological modelers [10–16]. The question arises what are the mechanisms that could generate such persistences. Mandelbrot [11] and Mandelbrot and Van Ness [12] pointed out that such behaviors arise in a class of processes with infinite memory, termed by them fractional Brownian noises (fB's). A hydrological interpretation of fB's was offered by Mandelbrot and Wallis [13]. Klemeš [14] argued that the Hurst phenomenon cannot be attributed to one specific physical cause. It can be caused by infinite memory of a particular type [11–13] or can be the result of nonstationarity in the process central tendency [14], and there may perhaps be other causes as well. One of the present authors and coworkers have suggested formulating the Hurst phenomenon from a dynamical systems point of view [17]. This idea is of relevance since, fundamentally, the laws governing the evolution of natural systems are deterministic. The question arises then, whether there exist deterministic models that generate statistical properties differing qualitatively from those associated to iidrv's possibly leading to the Hurst phenomenon.

In this paper, we introduce a general framework for analyzing the probabilistic properties of cumulative sums Eq. (2) and the (scaled) range Eq. (3) in deterministic dynamical systems. We start in Sec. II with some probabilistic aspects of the nonadjusted sums [i.e., without subtracting $\bar{X}_n$ in Eq. (1)]. Although this is a very simplified study, it enables us to get some first insights on the principal signatures of deterministic dynamics on the range analysis. In Secs. III and IV this initial study is extended to the case of adjusted sums as they appear in Eqs. (1) and (2). We develop a theory for the evaluation of the distribution $F(u,v,n)$ for deterministic dynamical systems. In sharp contrast with the classical theory of Feller [10], it turns out that $F(u,v,n)$ possesses nondiffer-

entiable points. In addition, we show that the densities $p(r_n)$ and $p^*(r_n^*)$ are discontinuous on a set of points that becomes dense when $n \to \infty$. Analysis of small-n cases complemented with numerical simulations entirely confirm our theory. The main conclusions are drawn in Sec. V.

II. PROBABILISTIC PROPERTIES OF THE NONADJUSTED SUMS IN DETERMINISTIC DYNAMICAL SYSTEMS

In order to sort out in a transparent way the type of effects that could arise in the presence of deterministic dynamics we first focus on the nonadjusted sums

$$\tilde{S}_1 = X_0, \tilde{S}_2 = X_0 + X_1, \ldots, \tilde{S}_n = X_0 + \ldots + X_{n-1}. \tag{5}$$

Let f be the dynamical law linking two successive values of the record

$$X_{i+1} = f(X_i), \quad X \in I = [a,b], \tag{6}$$

where I is a certain domain in phase space. In principle both X and f are vector quantities, since the instantaneous state of the system is typically determined by the values of more than one observable. We here assume that f can actually be contracted to a scalar form through, for instance, projection of the full dynamics on a Poincaré surface of section and/or the adiabatic elimination of fast variables. This entails, in particular, that f will be in general noninvertible.

In what follows, we will be interested in dynamical systems possessing sufficiently strong ergodic properties, such as systems generating deterministic chaos. Let $\rho_X^{(n)}(X_0, \ldots, X_{n-1})$ be the n-fold probability density of the sequence. In all generality, it can be decomposed into a product of the initial state density $\rho_X(X_0)$ which will be a smooth function of the variable X_0 and of a conditional probability density for going through the states $X_1, \ldots, X_{n-1}$ starting from X_0. In a deterministic system these conditional densities are δ-functions linking X_1 to X_0, X_2 to X_1, etc… [4],

$$\rho_X^{(n)}(X_0, \ldots, X_{n-1}) = \rho_X(X_0)\delta[X_1 - f(X_0)] \ldots \times \delta[X_{n-1} - f^{(n-1)}(X_0)], \tag{7}$$

where the superscript in $f^{(i)}$ denotes the ith iterate of f. It follows that the probability density of $\tilde{S}_n$ is

$$\rho(\tilde{S}_n) = \int_{I^n} dX_0 \ldots dX_{n-1} \rho_X^{(n)}(X_0, \ldots, X_{n-1}) \times \delta\left[\tilde{S}_n - \sum_{r=0}^{n-1} f^{(r)}(X_0)\right], \tag{8}$$

being understood that $f^{(0)}(X_0) = X_0$. Performing the integration over the space I^{n-1}, we get

$$\rho(\tilde{S}_n) = \int_I dX_0 \rho_X(X_0) \delta\left[\tilde{S}_n - \sum_{r=0}^{n-1} f^{(r)}(X_0)\right]. \tag{9}$$

Notice that Eq. (9) can also be viewed as the probability density that a certain function of the intial record X_0 has attained a "threshold" given by $\tilde{S}_n$.

Let $\{X_{0,\alpha}\}$ be the set of the preimages of $\tilde{S}_n$ under the mapping $\phi_n = \Sigma_{r=0}^{n-1} f^{(r)}(X_0)$, i.e. $X_{0,\alpha}$ is a solution of the equation

$$\sum_{r=0}^{n-1} f^{(r)}(X_0) = \tilde{S}_n. \tag{10a}$$

It then follows from Eq. (9) that

$$\rho(\tilde{S}_n) = \sum_\alpha \frac{\rho_X(X_{0,\alpha})}{\left|\sum_{r=0}^{n-1} f^{(r)'}(X_{0,\alpha})\right|}, \tag{10b}$$

where the denominator arises from the transformation of variables converting the δ-function in Eq. (9) to a product of δ-functions of the form $\delta(X_0 - X_{0,\alpha})$. As a rule, as $\tilde{S}_n$ is increased, the number of solutions $X_{0,\alpha}$ contributing to Eq. (10b) will change when crossing certain boundaries separating different $\tilde{S}_n$-values. This should result in a steplike form of $\rho(\tilde{S}_n)$.

As an elementary example consider the case of a window $n=2$ and a deterministic dynamics driven by the tent map [18], $f(X) = 1 - |1 - 2X|$, $0 \le X \le 1$. Notice that X is here nonnegative. There are no fundamental changes arising from this property as compared to the usual setting in which one deals with variables having a zero expectation, since one can subtract the ergodic average from each of the X_j's. We have

$$\tilde{S}_2 = \begin{cases} 3X_0, & \text{for } X_0 \in \left[0, \frac{1}{2}\right] \\ 2 - X_0, & \text{for } X_0 \in \left[\frac{1}{2}, 1\right] \end{cases}. \tag{11}$$

Alternatively [see Fig. 1 (top)],

$$\begin{aligned} X_{0,1} &= \tfrac{\tilde{S}_2}{3}, && \text{for } \tilde{S}_2 \in [0,1], \\ X_{0,1} &= \tfrac{\tilde{S}_2}{3}, X_{0,2} = 2 - \tilde{S}_2, && \text{for } \tilde{S}_2 \in \left(1, \tfrac{3}{2}\right], \end{aligned} \tag{12}$$

and Eq. (10b) yields, remembering that $\rho_X(X_0) = 1$ for the tent map,

$$\rho(\tilde{S}_2) = \begin{cases} \frac{1}{3}, & \text{for } \tilde{S}_2 \in [0,1] \\ \frac{4}{3}, & \text{for } \tilde{S}_2 \in \left(1, \frac{3}{2}\right] \end{cases}, \tag{13}$$

which has a steplike structure with a step occurring at $\tilde{S}_2 = 1$. This result is in full agreement with the results of numerical simulation of the full process, as summarized in Fig. 1 (bottom).

Building on the above analysis we may formally express the entire set of probabilities and probability densities relevant for the process, as summarized below.

A. Cumulative probability distribution

Let $\tilde{M}_n = \max(\tilde{S}_1, \ldots, \tilde{S}_n)$ and $\tilde{m}_n = \min(\tilde{S}_1, \ldots, \tilde{S}_n)$. Analogously to Eq. (7), the n-time probability density that the $n-1$ cumulative sums of the record following the state $\tilde{S}_1 = X_0$ are $\tilde{S}_2, \ldots, \tilde{S}_n$, respectively, is

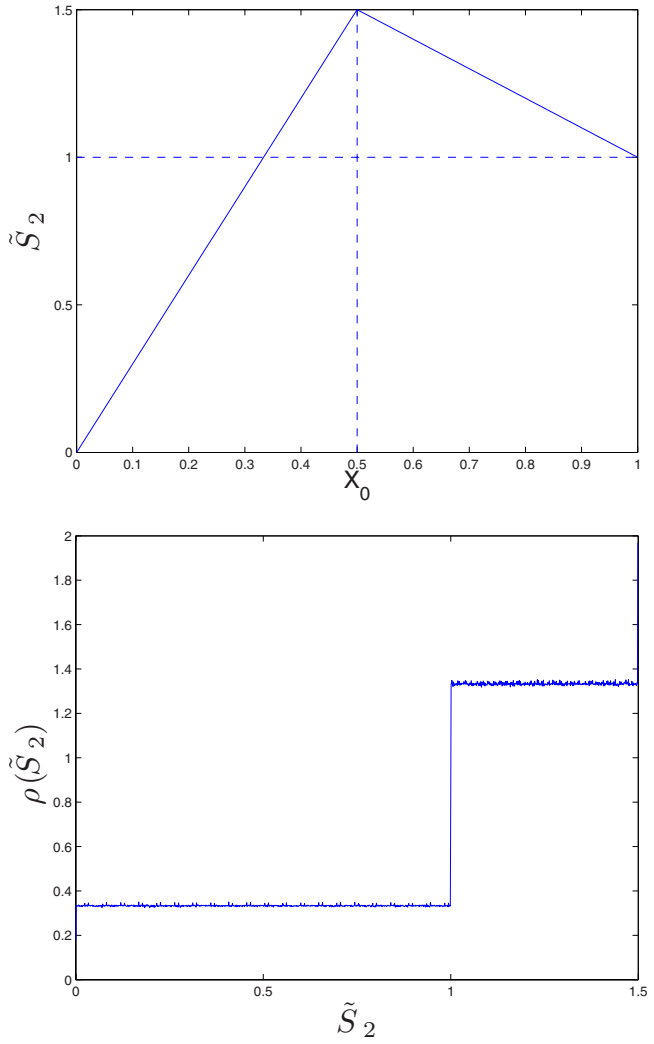

FIG. 1. (Color online) Top: nonadjusted sum $\tilde{S}_2$ for the tent map as a function of the initial state X_0 (solid line). Bottom: probability density $\rho(\tilde{S}_2)$ as obtained numerically using 10^6 realizations.

$$\rho^{(n)}(\tilde{S}_1,\ldots,\tilde{S}_n) = \rho(\tilde{S}_1)\prod_{i=1}^{n-1}\delta\left[\tilde{S}_{i+1} - \sum_{r=0}^{i} f^{(r)}(\tilde{S}_1)\right]. \quad (14)$$

By definition, the associated cumulative probability distribution is

$$F(u,v,n) = \mathrm{Prob}(\tilde{M}_n \le u, \tilde{m}_n \ge -v, n) = \int_{-v}^{u} d\tilde{S}_1 \ldots \int_{-v}^{u} d\tilde{S}_n \rho^{(n)}(\tilde{S}_1,\ldots,\tilde{S}_n). \quad (15)$$

A noteworthy difference with Eq. (4) is that in the present situation we may have $v<0$ since, e.g. in the tent map, $\tilde{S}_i>0$, although it should be kept in mind that $u>-v$. Eq. (15) can be further expressed in terms of Heaviside functions

$$F(u,v,n) = \int_{-v}^{u} d\tilde{S}_1 \rho(\tilde{S}_1)\prod_{i=1}^{n-1}\left\{H\left[u - \sum_{r=0}^{i} f^{(r)}(\tilde{S}_1)\right] - H\left[-v - \sum_{r=0}^{i} f^{(r)}(\tilde{S}_1)\right]\right\}. \quad (16)$$

Notice that in view of Eqs. (5) and (6) the domain of variation of $\tilde{S}_1$ is the interval I. Eq. (16) holds therefore as long as u is smaller than the upper boundary, b, and $-v$ larger than the lower boundary, a, of this interval. If either of these conditions is not fulfilled the upper and lower limits in the $\tilde{S}_1$ integration need to be replaced by b and a, respectively.

As, say, u is gradually increased keeping v constant, different Heaviside functions will "fire," resulting in an increasing function of u whose slope will suddenly change as new Heaviside functions will be becoming active. This will result in a dependence of F on u in the form of a broken line.

B. Density function

The probability density associated to $F(u,v,n)$ is $f(u,v,n)=F_{uv}(u,v,n)$. If $u<b$ we have

$$F_u = \rho(u)\prod_{i=1}^{n-1}\left\{H\left[u - \sum_{r=0}^{i} f^{(r)}(u)\right] - H\left[-v - \sum_{r=0}^{i} f^{(r)}(u)\right]\right\} + \int_{-v}^{u} d\tilde{S}_1 \rho(\tilde{S}_1)\sum_{i=1}^{n-1}\delta\left[u - \sum_{r=0}^{i} f^{(r)}(\tilde{S}_1)\right] \times \prod_{\substack{j=1 \\ j\neq i}}^{n-1}\left\{H\left[u - \sum_{r=0}^{j} f^{(r)}(\tilde{S}_1)\right] - H\left[-v - \sum_{r=0}^{j} f^{(r)}(\tilde{S}_1)\right]\right\}. \quad (17)$$

Clearly, the action of the derivative in Eq. (17) over v will result in δ-function singularities that cannot be regularized by subsequent integration over $\tilde{S}_1$. Notice that if $u>b$ only the second term in Eq. (17) with upper limit replaced by b will survive in the expression of F_u.

C. Probability density of the range

Following the classical work of Feller [10], the corresponding probability density of the range $\tilde{r}_n=\tilde{M}_n-\tilde{m}_n$ is

$$p(\tilde{r}_n) = \int_0^{\tilde{r}_n} du f(u,\tilde{r}_n - u, n), \quad (18)$$

and the tendency will be to regularize some of the δ-singularities of $f(u,v,n)$. Actually, $n=3$ is the minimal window for which a finite jump can be observed as $\tilde{r}_3$ is varied. As it turns out, $p(\tilde{r}_3)$ is then identical to $\rho(X_1+X_2)$ and thus has a structure identical to $\rho(\tilde{S}_2)$, see Eq. (13) and Fig. 1 for the example of the tent map.

III. SIGNATURE OF DETERMINISTIC DYNAMICS IN THE PROBABILITY $F(u,v,n)$ FOR ADJUSTED SUMS

A. General formulation of the probability $F(u,v,n)$

Having seen how deterministic dynamics may affect the probabilistic properties of cumulative sums of successive values of an observable, we turn to the properties of the adjusted partial sums S_j as they appear in the Hurst phenomenon per se, Eqs. (1), (2), (3a), and (3b). The definitions of the cumulative distribution Eq. (15) and the density of the range Eq. (18) evidently apply to adjusted partial sums as well. Technically, the main difference with the situation in the previous section is that for any given window n each of the partial sums depends now on the entire set of values of the record,

$$S_i = X_0 + \ldots + X_{i-1} - \frac{i}{n}(X_0 + \ldots + X_{n-1}). \tag{19}$$

Applying this equation to $i=1$ and rearranging terms we obtain

$$S_1 = X_0 - \frac{1}{n}\sum_{r=0}^{n-1} f^{(r)}(X_0) \equiv \psi_n^{(1)}(X_0), \tag{20a}$$

$$S_i = i(S_1 - X_0) + \sum_{r=0}^{i-1} f^{(r)}(X_0) \equiv \psi_n^{(i)}(X_0). \tag{20b}$$

As can be seen, S_1 can no longer be identified to X_0 and, as a corollary, there is no straightforward relation linking S_i to S_1. As a matter of fact, since $f(X_0)$ and thus $\psi_n^{(1)}(X_0)$ are generally noninvertible, there exist several solutions $\{X_{0,\alpha}\}$ of Eq. (19) expressed in terms of the various branches α of the inverse mapping $\psi_n^{(1)}$,

$$X_{0,\alpha} = (\psi_n^{(1)})_\alpha^{-1}(S_1). \tag{21}$$

Substitution into Eq. (20b) shows that S_j is, typically, a multivalued function of S_1 depending on the domain I_α of X_0-values associated to branch α of the inverse mapping in Eq. (21). We denote

$$S_{i,\alpha} = \psi_n^{(i)}(X_{0,\alpha}) \equiv g_\alpha^{(i-1)}(S_1), \tag{22}$$

where we have removed the reference to "n" for notational simplicity.

We now turn to the general formulation of the probabilistic properties of the S_j's. We start with the n-fold probability density $\rho^{(n)}(S_1,\ldots,S_n)$ that the $n-1$ adjusted cumulative sums following $S_1=x_0$ be $S_2,\ldots,S_n$. We partition the domain I of the original map f into m subintervals, each containing one of the preimages $X_{0,\alpha}$ of S_1 in Eq. (21). The boundaries between these intervals mark the switching between different expressions of $X_{0,\alpha}$ as a function of S_1, as S_1 runs over its interval of variation. For maps like the symmetric tent map considered in Sec. II these boundaries are, for a given n, the points $\alpha/2^n$, $\alpha=1,\ldots,2^n-1$ and the corresponding cells I_α define a Markov partition. For more general maps the subdivision is less obvious and one needs then to argue in terms of S_1, rather than X_0. Summarizing, we are led to the following formal expression:

$$\rho^{(n)}(S_1,\ldots,S_n) = \sum_{\alpha=1}^{m} P(X_0 \in I_\alpha)\rho_\alpha(S_1) \times \prod_{i=1}^{n-1} \delta[S_{i+1} - g_\alpha^{(i)}(S_1)], \tag{23}$$

where $\rho_\alpha(S_i)$ represents the conditional density $\rho(S_i|X_0 \in I_\alpha)$. Upon using the definition of the cumulative probability, given in Eq. (15), we get

$$F(u,v,n) = \sum_{\alpha=1}^{m} P(X_0 \in I_\alpha)F_\alpha(u,v,n), \tag{24}$$

where

$$\begin{aligned} F_\alpha(u,v,n) &= \int_{-v}^{u} dS_1 \rho_\alpha(S_1) \int_{-v}^{u} dS_2 \ldots \int_{-v}^{u} dS_n \\ &\quad \times \prod_{i=1}^{n-1} \delta[S_{i+1} - g_\alpha^{(i)}(S_1)] \\ &= \int_{-v}^{u} dS_1 \rho_\alpha(S_1) \prod_{i=1}^{n-1} \{H[u - g_\alpha^{(i)}(S_1)] \\ &\quad - H[-v - g_\alpha^{(i)}(S_1)]\}. \end{aligned} \tag{25}$$

In other words, $F_\alpha(u,v,n)$ is obtained by integrating $\rho_\alpha(S_1)$ over those ranges of S_1 in which $-v \le g_\alpha^{(i)}(S_1) \le u$, for $i=1,\ldots,n-1$.

Note that $g_\alpha^{(n-1)}(S_1)=0$ because $S_n=0$. Consequently, the last factor in Eq. (25), i.e. for $i=n-1$, reduces to $H(u)-H(-v)=1$ since we have by definition $u,v>0$. This means that for the practical computation of $F(u,v,n)$ it is not needed to take S_n into account, so we may consider $\rho^{(n-1)}(S_1,\ldots,S_{n-1})$ instead of $\rho^{(n)}(S_1,\ldots,S_n)$.

B. Application: $F(u,v,3)$ for fully developed chaos

We now turn to the application of the foregoing formalism to maps of the unit interval that exhibit fully developed chaos. We continue with the tent map as an illustrative example. We consider the simplest case $n=3$, dividing $I=[0,1]$ in subintervals $I_\alpha=[(\alpha-1)/4,\alpha/4]$, $\alpha=1,\ldots,4$. We recall that the tent map process is uniformly distributed, so that $P(X_0 \in I_\alpha)=1/4$ in Eq. (24). To obtain the overall structure of $F(u,v,3)$, we need the expressions for $F_i(u,v,3)$, $i=1,\ldots,4$, which are calculated below.

In line with the procedure presented in Eq. (20), we obtain S_1 and S_2 as a function of X_0, see Appendix A, Eqs. (A2) for details. The preimages $\{X_{0,\alpha}\}$ of S_1 under the mapping Eqs. (20a) are

$$\begin{aligned} &X_{0,1} = -\tfrac{3}{4}S_1, \quad X_{0,2} = \tfrac{3}{4}S_1 + \tfrac{1}{2}, \quad \text{for } S_1 \in \left[-\tfrac{1}{3},0\right], \\ &X_{0,4} = \tfrac{3}{8}S_1 + \tfrac{3}{4}, \qquad\qquad\qquad\quad \text{for } S_1 \in \left(0,\tfrac{2}{3}\right]. \end{aligned} \tag{26}$$

As seen in Eq. (22), we can write S_2 as a function of S_1 by substituting Eqs. (26) in S_2. We get

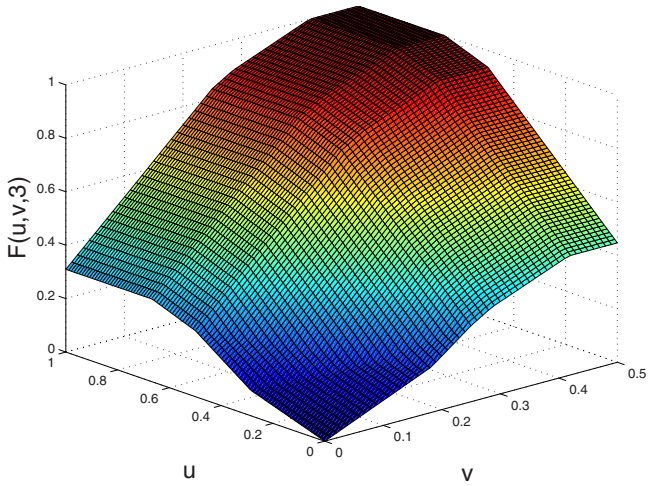

FIG. 2. (Color online) $F(u,v,3)$ for the tent map.

$$g_1^{(1)}(S_1) = \tfrac{5}{4}S_1, \quad g_2^{(1)}(S_1) = \tfrac{11}{4}S_1 + \tfrac{1}{2}, \quad \text{for } S_1 \in \left[-\tfrac{1}{3},0\right],$$
$$g_4^{(1)}(S_1) = \tfrac{7}{8}S_1 - \tfrac{1}{4}, \quad \text{for } S_1 \in \left(0,\tfrac{2}{3}\right]. \tag{27}$$

The case $X_0 \in I_3$ deserves some special attention because then $S_1=0$, so that S_2 cannot be written as a function of S_1. This is an exceptional situation not covered by the general formulation proposed in Sec. III A. The term for $\alpha=3$ in the sum Eq. (23) has then to be replaced by $1/4\,\delta(S_1)\rho_3(S_2)\delta(S_3)$.

The conditional densities, $\rho_\alpha(S_i)$, in Eqs. (23) and (25) are easily calculated: since X_0 is uniformly distributed, S_1 in Eq. (A2a) is then also uniformly distributed in each subinterval I_α. The conditional densities are thus block functions with surface equal to one. They can be expressed as a product of Heaviside functions,

$$\rho_1(S_1) = 3H\left(S_1 + \frac{1}{3}\right)H(-S_1), \tag{28a}$$

$$\rho_2(S_1) = \rho_1(S_1), \tag{28b}$$

$$\rho_3(S_2) = \frac{4}{3}H\left(S_2 + \frac{1}{4}\right)H\left(\frac{1}{2} - S_2\right), \tag{28c}$$

$$\rho_4(S_1) = \frac{3}{2}H(S_1)H\left(\frac{2}{3} - S_1\right). \tag{28d}$$

The conditions $-v \le g_1^{(1)}(S_1) \le u$, where $g_1^{(1)}(S_1)$ is given in Eqs. (27), are equivalent to $-4/5v \le S_1 \le 4/5u$. We find

$$F_1(u,v,3) = \int_{-4/5v}^{4/5u} dS_1 \rho_1(S_1), \tag{29}$$

which is equal to Eq. (B3) in Appendix B. For $F_2(u,v,3)$, the conditions $-v \le g_2^{(1)}(S_1) \le u$, where $g_2^{(1)}(S_1)$ is given in Eqs. (27), are equivalent to $-4/11v - 2/11 \le S_1 \le 4/11u - 2/11$. Actually, the computation of $F_2(u,v,3)$ is more complicated than the foregoing. Firstly, when $-4/11v - 2/11 < -v$ we have to consider $-v$ as the lower bound of the integration procedure,

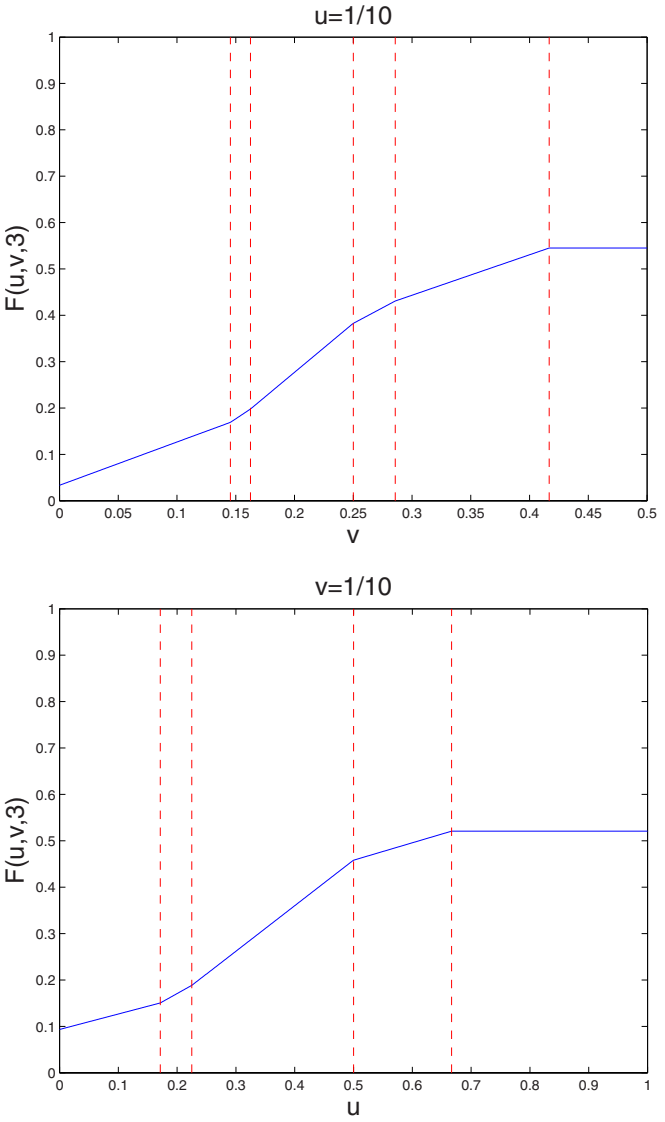

FIG. 3. (Color online) Solid line: $F(u,v,3)$ for the tent map as a function of v (top) or u (bottom), where u (top) or v (bottom) is kept constant. The broken lines indicate the nondifferentiable points. The plots are deduced numerically using 10^6 realizations and mesh size 0.01.

because otherwise, the integration range will be widened. Secondly, a restriction to the u- and v-values has to be imposed because it may happen that the lower bound $-4/11v - 2/11$ is larger than the upper bound $4/11u - 2/11$. This should imply that $F_2(u,v,3)$ is negative. This happens when $4/11u - 2/11 + v < 0$. Putting everything together yields Eq. (B4), see Appendix B. Similar computations give Eqs. (B5) and (B6).

From these expressions we can see that nondifferentiable points are located at $u=1/2$, $u=2/3$, $v=1/4$, $v=2/7$, and $v=5/12$. A three-dimensional plot of $F(u,v,3)$ is shown in Fig. 2. In addition, Fig. 3 displays the results for $F(u,v,3)$ by numerical simulation where we kept $u=1/10$ (or $v=1/10$) constant. This kind of two-dimensional plots provides actually a better visualization of the nondifferentiable points. Beside the above mentioned critical values, it

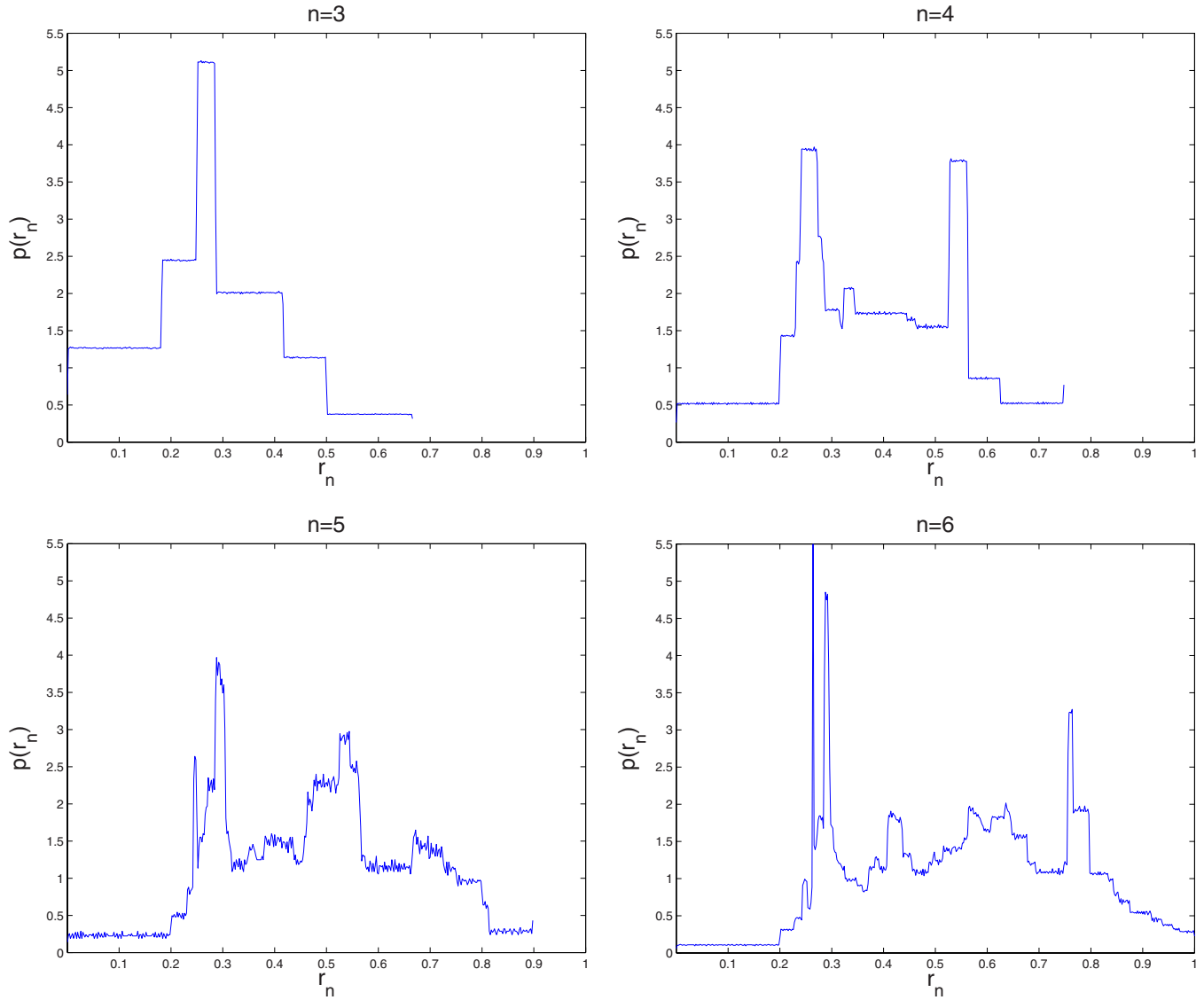

FIG. 4. (Color online) Probability density $p(r_n)$ for the tent map (small n) deduced numerically using 10^6 realizations and a mesh size $\Delta r_n = 0.01$.

can be seen that there are extra nondifferentiable points when keeping $u = 1/10$. They find their origins in the last Heaviside function of $F_2(u,v,3)$ and $F_4(u,v,3)$ since they vanish for $v = 8/55$ and $v = 13/80$, respectively. But as soon as u increases, this type of critical values are no longer present. An analogous remark holds for fixed v-values.

IV. SIGNATURE OF DETERMINISTIC DYNAMICS IN THE PROBABILITY DENSITY OF THE RANGE OF ADJUSTED SUMS

A. General formulation of the probability density of the range

The probability density of the range of adjusted sums can be obtained by suitably adapting the definitions of Secs. II B and II C to our case. It is recalled that the general form of $F(u,v,n)$ is given by Eqs. (24) and (25). Obviously, we have that

$$f(u,v,n) = \sum_{\alpha=1}^{m} P(X_0 \in I_\alpha) f_\alpha(u,v,n), \tag{30a}$$

where

$$f_\alpha(u,v,n) = (F_\alpha)_{uv}(u,v,n), \tag{30b}$$

and

$$p(r_n) = \sum_{\alpha=1}^{m} P(X_0 \in I_\alpha) p_\alpha(r_n), \tag{31a}$$

where

$$p_\alpha(r_n) = \int_0^{r_n} f_\alpha(u, r_n - u, n) du. \tag{31b}$$

Now we are able to explicitly compute $p(r_n)$ by introducing Eqs. (24) and (25) in Eqs. (30) and (31). The resulting computations are cumbersome, and they are listed in Appendix

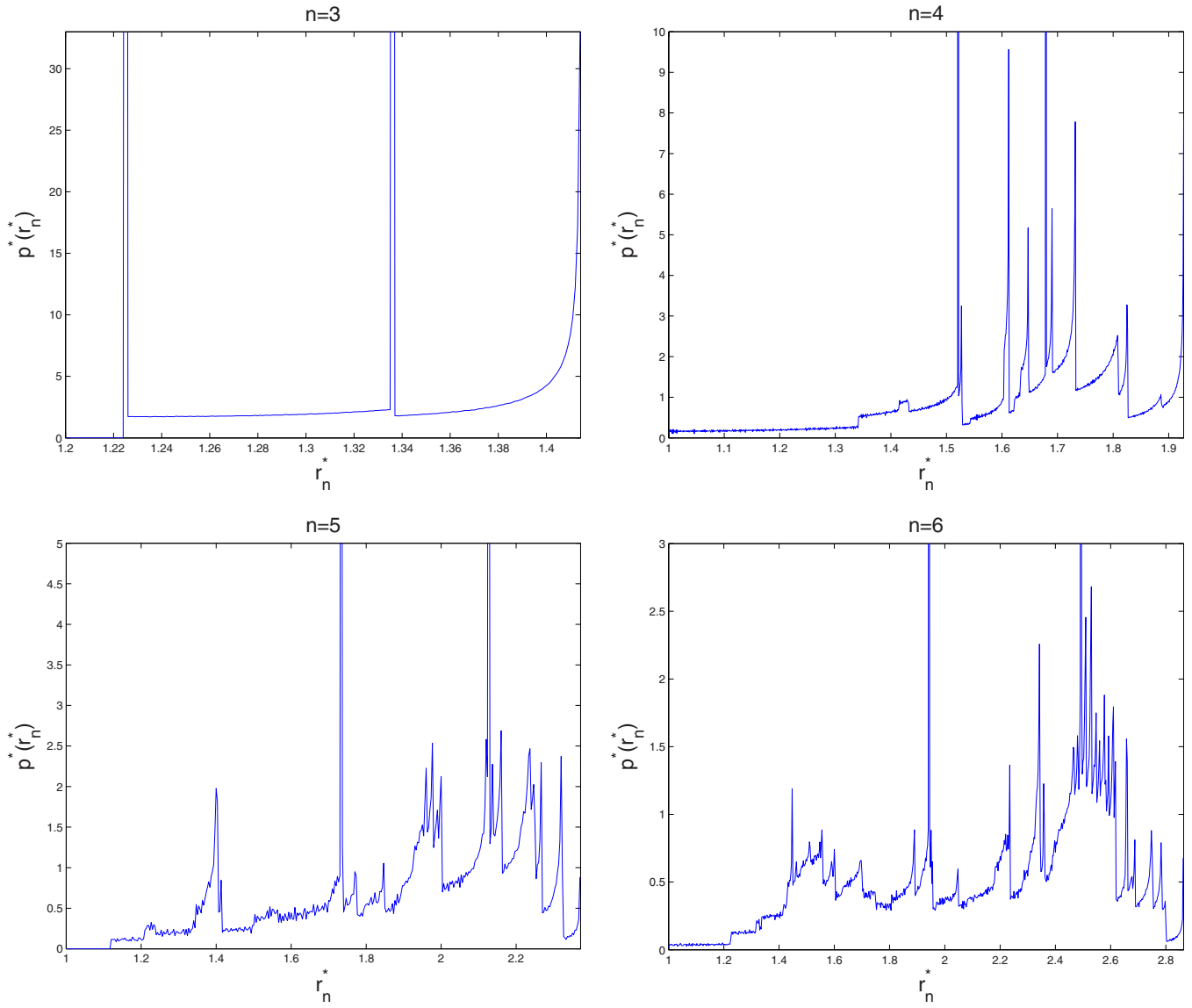

FIG. 5. (Color online) Probability density $p^*(r_n^*)$ for the tent map (small n) deduced numerically using 10^6 realizations and a mesh size $\Delta r_n^*=0.01$.

C. In sharp contrast with the classical theory, the occurring Heaviside functions in Eqs. (C3) and (C5) indicate that $p(r_n)$ possesses discontinuities. There is an additional reason for the existence of discontinuities in $p(r_n)$: it usually happens that the conditional densities $p_\alpha(r_n)$ in Eqs. (C3) and (C5) are nonzero at their endpoints and they are thus directly responsible for the jumps in the overall density $p(r_n)$. In Sec. IV B a detailed evaluation of $p(r_n)$ will be carried out on representative classes of chaotic dynamics.

When evaluating Eqs. (C3) and (C5) on concrete dynamical systems, it may happen that the undetermined form "$H(0)$" appears. Another additional shortcoming of the general formulation is that it does not provide any information on the probability density $p^*(r_n^*)$ of the scaled range. Unfortunately, the paper of Feller [10] does not deal with the scaled range r_n^* since it was assumed there that $C_n=1$. All these reasons justify that for the practical computation of $p(r_n)$ and $p^*(r_n^*)$, it should be desirable to search for an alternative construction procedure. This is illustrated in Sec. IV B 1.

B. Properties of $p(r_n)$ and $p^*(r_n^*)$: A case study

1. Small n-values

In Figs. 4 and 5 we have plotted the densities $p(r_n)$ and $p^*(r_n^*)$ for small n-cases $n=3,\ldots,6$ as obtained by direct numerical simulations using 10^6 realizations. Here, we intend to find some closed analytical expressions for $p(r_n)$ and $p^*(r_n^*)$ for window $n=3$, which is the smallest nontrivial case.

By construction of r_n, we can divide the system's domain I in nonintersecting successive subintervals J_α (not to be confused with the aforementioned I_α) in such a way that, in each J_α we have that $r_n=S_k(X_0)-S_l(X_0)$ for fixed k- and l-values. An illustrative example for r_3, which can be checked straightforwardly, is given in Eqs. (A3), see Appendix A. As can be seen from these expressions we have that r_3

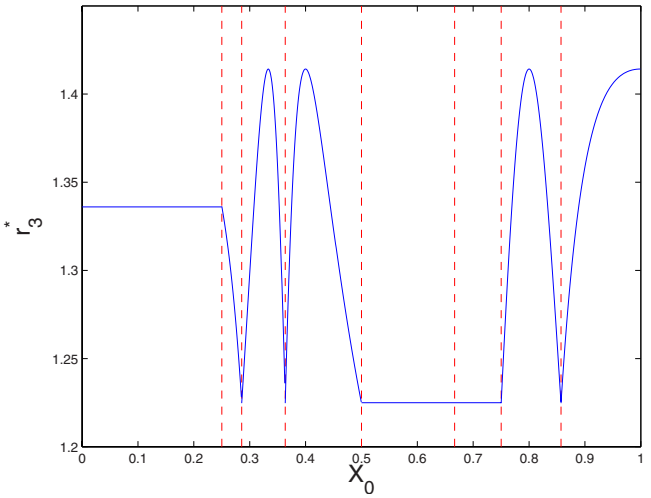

FIG. 6. (Color online) Scaled range r_3^* as a function of X_0 for the tent map. The broken lines divide the domain in the subintervals as listed in Eqs. (A3).

is a linear combination of X_0 in each J_α, and thus r_3 is uniformly distributed in J_α. Similar to the case of the conditional densities of the cumulative sums Eq. (28), we have consequently that the conditional densities $p(r_3|X_0 \in J_\alpha)$ are block functions. Then $p(r_n)$ can be easily obtained by using the law of total probability, see Eq. (A4) for the final outcome. Since each block function $p(r_3|X_0 \in J_\alpha)$ contributes to the overall density $p(r_3)$, we can see that the endpoints of $p(r_3|X_0 \in J_\alpha)$ may cause discontinuities in $p(r_3)$. The above features provide the insight that for the tent map, $p(r_n)$ is a linear combination of block functions. The number of block functions contributing to the overall density $p(r_n)$ increases as n becomes larger and larger. As a corollary, the number of discontinuous points becomes dense as $n \to \infty$.

We have not found an analytical expression for the density $p^*(r_3^*)$, but the expression of r_3^*, provided by Eqs. (A3) and (A1b), suggests some relevant conclusions on $p^*(r_3^*)$. In Fig. 6 we show r_3^* as a function of X_0. For $X_0 \in J_1$ we obtain that $r_3^* = 5/14^{0.5} \approx 1.336$, resulting in a contribution of a δ-function in $p^*(r_3^*)$. Indeed, we have that: $p^*(r_3^*|X_0 \in J_1) = \delta(r_3^* - 5/14^{0.5})$. Similarly, a second δ-peak is located at $r_3^* = (3/2)^{0.5} \approx 1.225$ when $X_0 \in J_5 \cup J_6$. Beside the occurring δ-functions, there is a jump at the right-endpoint of $p^*(r_3^*)$, here $r_3^* = \sqrt{2}$, because in J_3, J_4, J_7, and J_8, the function r_3^* reaches this maximum value. The minimum value, $r_3^* = (3/2)^{0.5}$, which is reached in every subinterval (except J_1), cannot cause a jump in $p^*(r_3^*)$ because there is a δ-peak located at that value. A similar situation happens in J_2 where the maximum value $r_3^* = 5/14^{0.5}$ at the left endpoint is reached. Fig. 5 (left, top) confirms our analysis.

2. Large n values

Next, we illustrate how $p^*(r_n^*)$ evolves for larger n values. We do not show the results for $p(r_n)$ because they are comparable to the previous ones. In Fig. 7 we have plotted the standardized probability density $p^*(r_n^*)$ for the tent map. For comparison, we used the uniformly distributed random process in the unit interval (i.e., the iidrv case) as reference. It should be noted that distribution in the iidrv case can also be approximated by the asymptotic results in [10] for uncorrelated data.

The results confirm entirely the persistence of discontinuities in accord with the theoretical predictions. Aside from these discontinuities in the probability density, we also observe that for moderate n values the standardized densities follow, remarkably enough, the main body of the standardized density in the iidrv case. We suggest that a qualitiative mechanism at the origin of this phenomenon is as follows. As seen in the previous subsection, individual r_n^*'s in the different subintervals of the domain of definition are differences of adjusted sums—or alternatively linear combinations of the original variables X_i evaluated at different times—normalized by the standard deviation C_n. This operation may be viewed as a filter [19] tending to smooth the variability of r_n^* relative to that of X. Still, gaps within and irregular pronounced oscillations around the overall smooth envelope

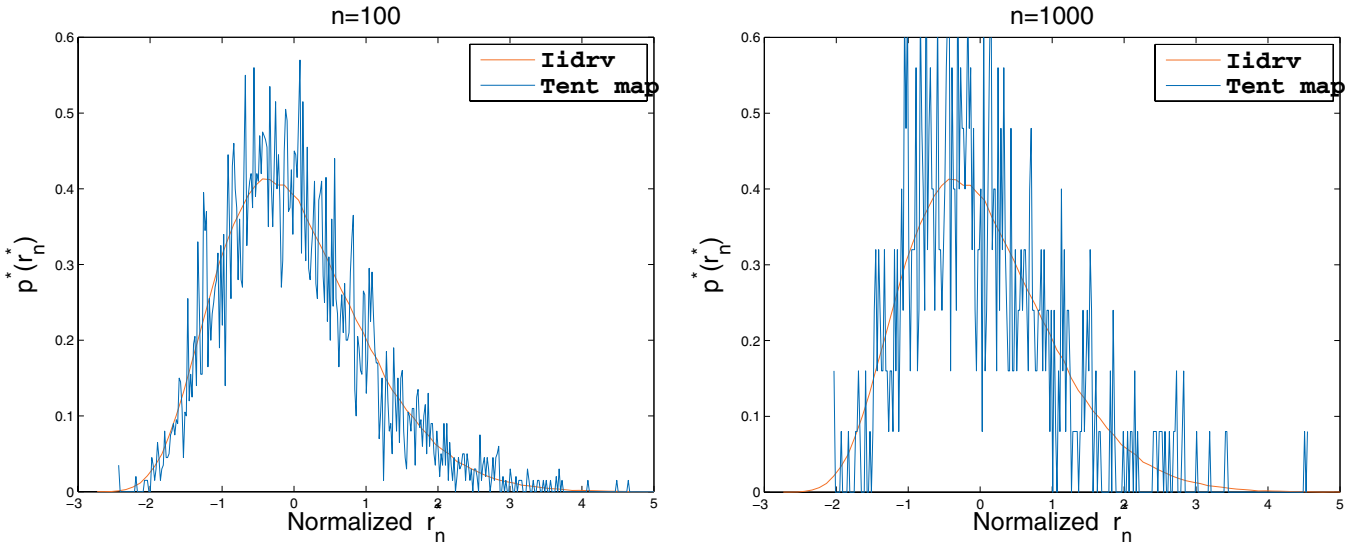

FIG. 7. (Color) Standardized probability density $p^*(r_n^*)$ deduced numerically using 10^4 realizations and a mesh size $\Delta r_n^* = 0.01$.

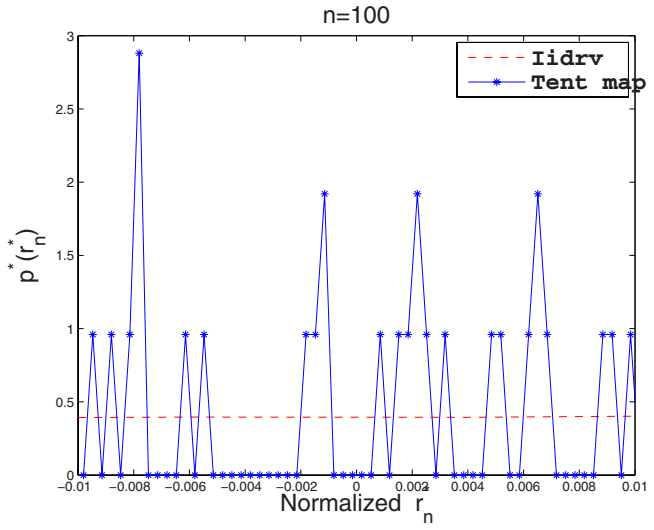

FIG. 8. (Color online) Zoomed standardized probability density $p^*(r_n^*)$ deduced numerically using 10^5 realizations and a mesh size $\Delta r_n^*=3.3310^{-4}$.

persist on small scales as shown in Fig. 8, where a zoom of the probability density for $n=100$ in a small part of the interval is shown. Interestingly, there are only three nontrivial density values in that interval. This variability is gradually erased at the level of locally averaged observables such as sliding means, as illustrated in Fig. 9 for an averaging window with 50 members.

The foregoing experiments have been carried out on the Bernoulli shift [18], $f(X)=2X \bmod 1$, $0\leq X\leq 1$, which is also a representative example of fully developed chaos. In the case of intermittent chaos we have considered the widely used cusp map [18], $f(X)=1-2|X|^{1/2}$, $|X|\leq 1$. The outcome of the numerical experiments (not shown here) is completely analogous to the results of the tent map.

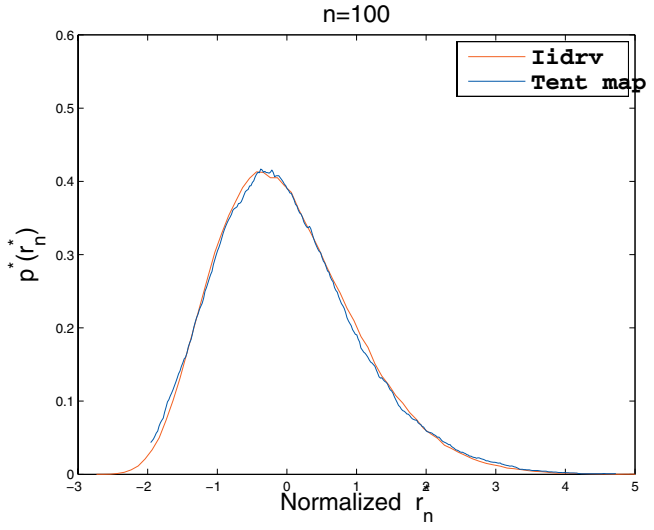

FIG. 9. (Color) Averaged probability density of r_n^*. The original density is taken from Fig. 7 (left) and the sliding averaging window contains 50 values.

V. CONCLUSIONS

In this work the basic quantities in the statistics of the range of sums, i.e., $F(u,v,n)$, $p(r_n)$, and $p^*(r_n^*)$ have been analyzed for deterministic dynamical systems. A general formulation of $F(u,v,n)$ and $p(r_n)$ was made possible by expressing the n-time probability density $\rho^{(n)}(S_1,\ldots,S_n)$ in a way analogous to the theory of extreme events in deterministic systems [4]. In sharp contrast with the Feller's classical theory [10] for iidrv's, we have shown that $F(u,v,n)$ contains nondifferentiable points. We have constructed the corresponding $p(r_n)$ and were able to explain the existence of discontinuous points in $p(r_n)$ and $p^*(r_n^*)$ using representative models of fully developed chaos. Furthermore, the number of discontinuities increases as n grows, thus no simple limiting behavior is to be expected. A noteworthy difference between $p(r_n)$ and $p^*(r_n^*)$ is that the latter distribution might contain δ functions.

Further work in this area should aim at determining the class of nonlinear phenomena that may generate behaviors similar to the Hurst phenomenon per se, i.e., $\langle r_n^* \rangle \sim n^H$. In the presence of intermittent chaos, initial encouraging results have already been reported in [17]. Similar experiments (in preparation) on the chaotic bimodal map [7] reveal a Hurst type power law within a large observational time window. Analogously to most stochastic processes, experiments on a variety of dynamical systems have shown a (sometimes very slow) convergence to $n^{0.5}$. One would be tempted to speculate that this conclusion should extend to all fully developed chaotic systems whose variables evolve according to a bounded and stationary process. One should then examine how the window beyond which the exponent H falls down to 0.5, is related to the presence of long range correlations in the system. Finally, it would be desirable to analyze the applicability of the new theory on realistic models describing hydrodynamic chaos or atmospheric circulation. This research is now in progress.

ACKNOWLEDGMENTS

H. Van de Vyver acknowledges numerous discussions with S. Vannitsem on extreme value theory. This work is supported, in part, by the Science Policy Office of the Belgian Government under Contract No. MO/34/017.

APPENDIX A: COMPUTATION AND STATISTICS OF r_3 FOR THE TENT MAP

For the data set X_0, X_1, X_2 generated by the tent map, we have the following statistics,

$$\bar{X}_3 = \begin{cases} \frac{7}{3}X_0, & X_0 \in [0,1/4] \\ -\frac{1}{3}X_0 + \frac{2}{3}, & X_0 \in [1/4,1/2] \\ X_0, & X_0 \in [1/2,3/4] \\ -\frac{5}{3}X_0 + 2, & X_0 \in [3/4,1] \end{cases}, \qquad \text{(A1a)}$$

and

$$C_3^2 = \begin{cases} \frac{14}{9}X_0^2, & X_0 \in [0,1/4] \\ \frac{62}{9}X_0^2 - \frac{44}{9}X_0 + \frac{8}{9}, & X_0 \in [1/4,1/2] \\ \frac{2}{3}(3X_0-2)^2, & X_0 \in [1/2,3/4] \\ \frac{38}{9}X_0^2 - \frac{20}{3}X_0 + \frac{8}{3}, & X_0 \in [3/4,1] \end{cases}. \quad \text{(A1b)}$$

After straightforward calculations, we obtain for the sums S_1 and S_2,

$$S_1 = \begin{cases} -\frac{4}{3}X_0, & X_0 \in [0,1/4] \\ \frac{4}{3}X_0 - \frac{2}{3}, & X_0 \in [1/4,1/2] \\ 0, & X_0 \in [1/2,3/4] \\ \frac{8}{3}X_0 - 2, & X_0 \in [3/4,1] \end{cases}, \quad \text{(A2a)}$$

and

$$S_2 = \begin{cases} -\frac{5}{3}X_0, & X_0 \in [0,1/4] \\ \frac{11}{3}X_0 - \frac{4}{3}, & X_0 \in [1/4,1/2] \\ -3X_0 + 2, & X_0 \in [1/2,3/4] \\ \frac{7}{3}X_0 - 2, & X_0 \in [3/4,1] \end{cases}. \quad \text{(A2b)}$$

The range of sums is then given by

$$r_3 = \begin{cases} S_3 - S_2 = \frac{5}{3}X_0, & X_0 \in [0,1/4] \\ S_3 - S_2 = -\frac{11}{3}X_0 + \frac{4}{3}, & X_0 \in [1/4,2/7] \\ S_3 - S_1 = -\frac{4}{3}X_0 + \frac{2}{3}, & X_0 \in [2/7,4/11] \\ S_2 - S_1 = \frac{7}{3}X_0 - \frac{2}{3}, & X_0 \in [4/11,1/2] \\ S_2 - S_3 = -3X_0 + 2, & X_0 \in [1/2,2/3] \\ S_3 - S_2 = 3X_0 - 2, & X_0 \in [2/3,3/4] \\ S_1 - S_2 = \frac{1}{3}X_0, & X_0 \in [3/4,6/7] \\ S_1 - S_3 = \frac{8}{3}X_0 - 2, & X_0 \in [6/7,1] \end{cases}. \quad \text{(A3)}$$

The procedure introduced in Sec. IV B 1 enables us to compute the density:

$$\begin{aligned} p(r_3) = {} & \frac{3}{5}\theta\left(\frac{5}{12} - r_3\right) + \frac{3}{11}\theta\left(-\frac{2}{7} + r_3\right)\theta\left(\frac{5}{12} - r_3\right) \\ & + \frac{3}{4}\theta\left(-\frac{2}{11} + r_3\right)\theta\left(\frac{2}{7} - r_3\right) + \frac{3}{7}\theta\left(-\frac{2}{11} + r_3\right) \\ & \times \theta\left(\frac{1}{2} - r_3\right) + \frac{1}{3}\theta\left(\frac{1}{2} - r_3\right) + \frac{1}{3}\theta\left(\frac{1}{4} - r_3\right) \\ & + 3\theta\left(-\frac{1}{4} + r_3\right)\theta\left(\frac{2}{7} - r_3\right) + \frac{3}{8}\theta^*\left(-\frac{2}{7} + r_3\right)\theta\left(\frac{2}{3} - r_3\right). \end{aligned} \quad \text{(A4)}$$

APPENDIX B: $F(u,v,3)$ FOR THE TENT MAP

The cumulative distribution function Eq. (4) for $n=3$ takes the form

$$F(u,v,3) = \frac{1}{4}\sum_{i=1}^{4} F_i(u,v,3). \quad \text{(B1)}$$

In what follows, we define the step functions θ and θ^* as

$$\theta(x) = \begin{cases} 1 & \text{if } x \geq 0 \\ 0 & \text{if } x < 0 \end{cases} \quad \text{and} \quad \theta^*(x) = \begin{cases} 1 & \text{if } x > 0 \\ 0 & \text{if } x \leq 0 \end{cases}, \quad \text{(B2)}$$

in order to have $F_i(u,v,3)=1$ at the endpoints. Definition (B2) will be used throughout this work.

The F_i's in Eq. (B1) are given by

$$F_1(u,v,3) = \frac{12}{5}v\,\theta\left(1 - \frac{12}{5}v\right) + \theta^*\left(-1 + \frac{12}{5}v\right), \quad \text{(B3)}$$

$$\begin{aligned} F_2(u,v,3) = {} & \left[\theta\left(\frac{2}{7} - v\right)F_2^{(1)} + \theta^*\left(-\frac{2}{7} + v\right)F_2^{(2)}\right] \\ & \times \theta\left(\frac{4}{11}u - \frac{2}{11} + v\right), \end{aligned} \quad \text{(B4a)}$$

where

$$\begin{aligned} F_2^{(1)} = {} & \int_{-v}^{4/11u-2/11} dS_1 \rho_2(S_1) \\ = {} & 3v\,\theta\left(\frac{1}{3} - v\right) + \theta^*\left(-\frac{1}{3} + v\right) + \frac{6}{11}(2u-1)\,\theta\left(\frac{1}{2} - u\right), \end{aligned} \quad \text{(B4b)}$$

and

$$\begin{aligned} F_2^{(2)} = {} & \int_{-4/11v-2/11}^{4/11u-2/11} dS_1 \rho_2(S_1) \\ = {} & \frac{6}{11}(2v+1)\,\theta\left(\frac{5}{12} - v\right) + \theta^*\left(-\frac{5}{12} + v\right) \\ & + \frac{6}{11}(2u-1)\,\theta\left(\frac{1}{2} - u\right), \end{aligned} \quad \text{(B4c)}$$

$$F_3(u,v,3) = \frac{4}{3}u\theta\left(\frac{1}{2}-u\right) + \frac{2}{3}\theta^*\left(-\frac{1}{2}+u\right) + \frac{4}{3}v\,\theta\left(\frac{1}{4}-v\right) + \frac{1}{3}\theta^*\left(-\frac{1}{4}+v\right), \tag{B5}$$

$$F_4(u,v,3) = \left[\frac{3}{2}u\theta\left(\frac{2}{3}-u\right) + \theta^*\left(-\frac{2}{3}+u\right) + \frac{3}{7}(-1+4v)\theta\left(\frac{1}{4}-v\right)\right]\theta\left(u+\frac{8}{7}v-\frac{2}{7}\right). \tag{B6}$$

APPENDIX C: GENERAL FORM OF $p(r_n)$

We compute $f_\alpha(u,v,n)$ by using Eqs. (25) and (30b),

$$(F_\alpha)_u = \rho_\alpha(u) \times \prod_{i=1}^{n-1} \{H[u-g_\alpha^{(i)}(u)] - H[-v-g_\alpha^{(i)}(u)]\} + \int_{-v}^{u} dS_1 \rho_\alpha(S_1) \sum_{i=1}^{n-1} \delta[u-g_\alpha^{(i)}(S_1)] \times \prod_{\substack{j=1 \\ j\neq i}}^{n-1} \{H[u-g_\alpha^{(j)}(S_1)] - H[-v-g_\alpha^{(j)}(S_1)]\}, \tag{C1}$$

and thus

$$\begin{aligned} f_\alpha = {} & \rho_\alpha(u) \sum_{i=1}^{n-1} \delta[-v-g_\alpha^{(i)}(u)] \\ & \times \prod_{\substack{j=1 \\ j\neq i}}^{n-1} \{H[u-g_\alpha^{(j)}(u)] - H[-v-g_\alpha^{(j)}(u)]\} + \rho_\alpha(-v) \sum_{i=1}^{n-1} \delta[u-g_\alpha^{(i)}(-v)] \\ & \times \prod_{\substack{j=1 \\ j\neq i}}^{n-1} \{H[u-g_\alpha^{(j)}(-v)] - H[-v-g_\alpha^{(j)}(-v)]\} + \int_{-v}^{u} dS_1 \rho_\alpha(S_1) \sum_{i=1}^{n-1} \delta[u-g_\alpha^{(i)}(S_1)] \sum_{\substack{j=1 \\ j\neq i}}^{n-1} \delta[-v-g_\alpha^{(j)}(S_1)] \\ & \times \prod_{\substack{k=1 \\ k\neq j, k\neq i}}^{n-1} \{H[u-g_\alpha^{(k)}(S_1)] - H[-v-g_\alpha^{(k)}(S_1)]\}. \end{aligned} \tag{C2}$$

Using Eq. (31b) we can write that $p_\alpha(r_n) = p_\alpha^{(1)}(r_n) + p_\alpha^{(2)}(r_n) + p_\alpha^{(3)}(r_n)$, where

$$\begin{aligned} p_\alpha^{(1)}(r_n) = {} & \int_0^{r_n} du \rho_\alpha(u) \sum_{i=1}^{n-1} \delta[u-r_n-g_\alpha^{(i)}(u)] \\ & \times \prod_{\substack{j=1 \\ j\neq i}}^{n-1} \{H[u-g_\alpha^{(j)}(u)] - H[u-r_n-g_\alpha^{(j)}(u)]\} \\ = {} & \sum_{i=1}^{n-1} \sum_{\eta_i} \frac{\rho_\alpha(u_\alpha^{(\eta_i)})}{|1-g_\alpha^{(i)\prime}(u_\alpha^{(\eta_i)})|} [H(r_n-u_\alpha^{(\eta_i)}) - H(-u_\alpha^{(\eta_i)})] \\ & \times \prod_{\substack{j=1 \\ j\neq i}}^{n-1} \{H[u_\alpha^{(\eta_i)} - g_\alpha^{(j)}(u_\alpha^{(\eta_i)})] \\ & - H[u_\alpha^{(\eta_i)} - r_n - g_\alpha^{(j)}(u_\alpha^{(\eta_i)})]\}, \end{aligned} \tag{C3}$$

and $\{u_\alpha^{(\eta_i)}\}$ are the solutions of the equation,

$$x - r_n - g_\alpha^{(i)}(x) = 0. \tag{C4}$$

Analogously, we have

$$\begin{aligned} p_\alpha^{(2)}(r_n) = {} & \int_0^{r_n} du \rho_\alpha(u-r_n) \sum_{i=1}^{n-1} \delta[u-g_\alpha^{(i)}(u-r_n)] \\ & \times \prod_{\substack{j=1 \\ j\neq i}}^{n-1} \{H[u-g_\alpha^{(j)}(u-r_n)] - H[u-r_n-g_\alpha^{(j)}(u-r_n)]\} \\ = {} & \sum_{i=1}^{n-1} \sum_{\xi_i} \frac{\rho_\alpha(u_\alpha^{(\xi_i)} - r_n)}{|1-g_\alpha^{(i)\prime}(u_\alpha^{(\xi_i)} - r_n)|} [H(r_n-u_\alpha^{(\xi_i)}) - H(-u_\alpha^{(\xi_i)})] \\ & \times \prod_{\substack{j=1 \\ j\neq i}}^{n-1} \{H[u_\alpha^{(\xi_i)} - g_\alpha^{(j)}(u_\alpha^{(\xi_i)} - r_n)] \\ & - H[u_\alpha^{(\xi_i)} - r_n - g_\alpha^{(j)}(u_\alpha^{(\xi_i)} - r_n)]\}, \end{aligned} \tag{C5}$$

where $\{u_\alpha^{(\xi_i)}\}$ are the solutions of the equation,

$$x - g_\alpha^{(i)}(x-r_n) = 0. \tag{C6}$$

We do not report $p_\alpha^{(3)}(r_n)$ because the expression is too long.

[1] E. J. Gumbel, *Statistics of Extremes* (Columbia University Press, New York, 1958).
[2] P. Embrechts, P. Klüppelberg, and T. Mikosch, *Modelling Extremal Events* (Springer, New York, 1997).
[3] M. Leadbetter and H. Rootzén, Ann. Probab. **16**, 431 (1988).
[4] V. Balakrishnan, C. Nicolis, and G. Nicolis, J. Stat. Phys. **80**, 307 (1995).
[5] C. Nicolis, V. Balakrishnan, and G. Nicolis, Phys. Rev. Lett. **97**, 210602 (2006).
[6] C. Nicolis and S. C. Nicolis, EPL **80**, 40003 (2007).
[7] S. C. Nicolis and C. Nicolis, Phys. Rev. E **78**, 036222 (2008).
[8] G. Nicolis, V. Balakrishnan, and C. Nicolis, Stochastics Dyn. **8**, 115 (2008).
[9] H. E. Hurst, Trans. Am. Soc. Civ. Eng. **116**, 770 (1951).
[10] W. Feller, Ann. Math. Stat. **22**, 427 (1951).
[11] B. B. Mandelbrot, C. R. Acad. Sci. Paris **260**, 3274 (1965).
[12] B. B. Mandelbrot and J. W. Van Ness, SIAM Rev. **10**, 422 (1968).
[13] B. B. Mandelbrot and J. R. Wallis, Water Resour. Res. **4**, 909 (1968).
[14] V. Klemeš, Water Resour. Res. **10**, 675 (1974).
[15] R. N. Bhattacharya, V. K. Gupta, and E. Waymire, J. Appl. Probab. **20**, 649 (1983).
[16] C. Yeung, M. Rao, and R. Desai, Phys. Rev. Lett. **73**, 1813 (1994).
[17] G. Nicolis and C. Nicolis, *Foundations of Complex Systems* (World Scientific Publishing Co. Pte. Ltd., Singapore, 2007).
[18] G. Nicolis, *Introduction to Nonlinear Science* (Cambridge University Press, Cambridge, England, 1995).
[19] A. Papoulis, *Signal Analysis* (McGraw-Hill, New York, 1984).